

**DOUBLE INTERPOLATION TO ACHIEVE LINEAR STRAIN PATH FOR AISI 1008 STEEL
CRUCIFORM SPECIMEN**

Jordan Hoffman
University of New
Hampshire
Durham, NH

Jinjin Ha
University of New
Hampshire
Durham, NH

Brad Kinsey
University of New
Hampshire
Durham, NH

Dilip Banerjee
National Institute of
Standards and
Technology
Gaithersburg, MD

Mark A. Iadicola
National Institute of
Standards and
Technology
Gaithersburg, MD

ABSTRACT

The automotive industry relies heavily on sheet metal forming processes for many components. Material data solely from uniaxial testing is insufficient to fully define the material behavior of the complex plastic deformation during numerical simulations of the forming processes. In-plane biaxial testing using a cruciform type specimen is a more comprehensive representation than the traditional uniaxial testing alone. Wide ranging biaxial stress states can be imposed by applying different loading conditions on each cruciform axis. However, this can create a challenge to achieve desired deformation paths due to the non-linear relationship between the control parameter, e.g., displacement, and the output of interest, e.g., strain path. In this paper, an interpolation method to develop the displacement control that produces a linear strain path with a desired strain ratio is revisited and expanded upon from the authors' previous work [1,2]. In the first iteration, linear biaxial displacements were applied to the specimen and the corresponding strain paths were obtained from the numerical simulations. The non-linear strain paths, due to geometry effects of the specimen, were used to reverse engineer a new displacement path that results in a linear strain path. Interpolation is revisited to show increased success with a second iteration. Analysis of the simulation results shows that linear strain paths of a given model can be determined and improved by successive iterations of interpolating the strain data from adjacent deformation paths.

1. INTRODUCTION

Sheet metal forming is known to produce high quantities of parts with consistent quality, notably for the automotive industry. The implementation of the forming process, however, can be challenging due to the lack of agreement between predictive simulations and actual process parts. This discrepancy is partially caused by using only uniaxial test data in the simulations to characterize the material behavior, which does not represent the multiaxial nature of the actual process. There is a

need to produce material data under various stress states to capture the complexities introduced by multiaxial deformation.

Biaxial tension testing using a cruciform specimen to produce multiaxial data could aid in the development of new or improved material models for forming simulations. In this test, specimens are loaded in two orthogonal directions in the plane of the sheet. Material response (i.e., force-displacement and strain data) can be collected via measurement systems, such as a load cell, displacement sensor, and digital image correlation (DIC) respectively [3]. Most in-plane biaxial tension machines operate using a prescribed signal-based control system, such as force or displacement. However, the applied deformation path to the control system does not guarantee the specific strain deformation in the gauge area that the user desires. This requires a method to systematically adjust the deformation path to be in a non-linear form. Some advanced systems feature real-time feedback controllers that can determine the path based on the deformed parameters, e.g., stress and strain [4]. However, these testing systems are more complicated, expensive, and less reliable when strain localization occurs (e.g., Lüders banding).

In previous work, a computational method called interpolation [1,2] was introduced to generate a non-linear displacement path necessary to produce a linear strain path with the desired strain ratio. This method utilizes two adjacent strain paths and a target as inputs, in correlation with their displacement paths.

This paper will outline the interpolation method and present results based on finite element (FE) simulations. It should be noted that the same approach can and will be used in the future to obtain experimental results. Double interpolation, i.e., processed twice, to achieve a strain path closer to the target with increased linearity than single iteration will also be demonstrated.

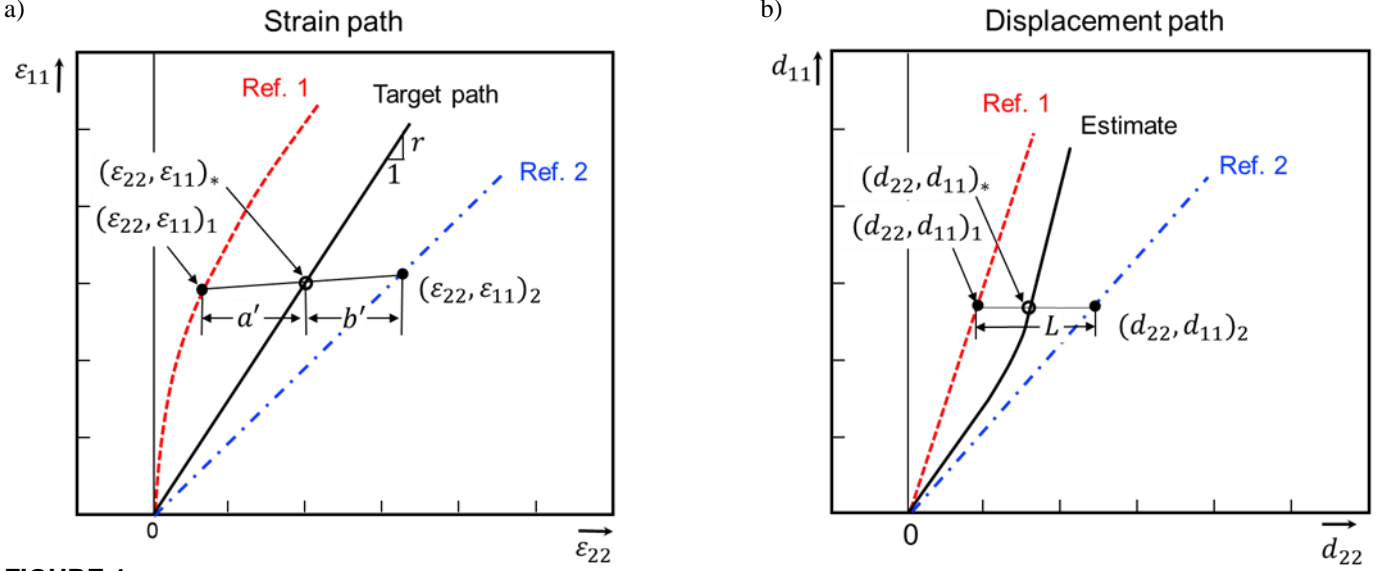


FIGURE 1: SCHEMATIC DESCRIPTION OF INTERPOLATION METHOD. a) DETERMINATION OF CORRECTION VARIABLES a' AND b' BASED ON TWO REFERENCE (REF) STRAIN CURVES (RED DASH AND BLUE DOT DASH) WITH TARGET RATIO (SOLID BLACK) IN BETWEEN. b) REFERENCE (REF) DISPLACEMENT PATHS AND RESULTING INTERPOLATED ESTIMATE FOR TARGET PATH.

2. INTERPOLATION METHOD

The interpolation method [1,2] requires two reference strain paths and a target linear strain path that will be the desired outcome. In this paper, initial reference curves were produced using linear input displacements in FE simulations (displacement ratios $d_{11}:d_{22}$ of 2:2, 2:1, 2:0.5, 2:-0.4, and 2:-0.8). The target path must lie in between two selected reference curves as shown in Figure 1a). If a reference path crosses the target path, another reference curve may be used beginning at the increment of intersection for the remainder of the interpolation. The strain path is comprised of two components, i.e., the major and the minor direction strains, ε_{11} and ε_{22} , respectively. Accordingly, the major direction displacement d_{11} , which is held linear throughout the simulations, and the minor direction displacement d_{22} , that is adjusted systematically (Figure 1b), are obtained.

A calculation is performed using the strain data from the reference curves. In this calculation, a theoretical line is formulated to connect strain levels on the reference curves at each time increment of the FE simulation. This is shown in Figure 1a as connecting two points on the reference paths. Since the theoretical line is connecting the reference paths, it also passes through the target path. The intersection between them can be expressed in terms of the strain components in the reference paths and the target ratio, or linear slope of the target path, by:

$$(\varepsilon_{22})_* = \frac{\left[(\varepsilon_{11})_2 - \frac{[(\varepsilon_{11})_2 - (\varepsilon_{11})_1]}{[(\varepsilon_{22})_2 - (\varepsilon_{22})_1]} \times (\varepsilon_{11})_2 \right]}{\left(r - \frac{[(\varepsilon_{11})_2 - (\varepsilon_{11})_1]}{[(\varepsilon_{22})_2 - (\varepsilon_{22})_1]} \right)} \quad (1)$$

where the subscripts 1, 2 and * refer to the left and right reference paths and a curve based on the target ratio ' r ', respectively. Thus, the strain components at the intersection can be calculated as

$(\varepsilon_{22}, \varepsilon_{11})_* = (\varepsilon_{22}, r \cdot \varepsilon_{22})_*$. A relationship is then established in terms of correction variables a' and b' to quantify the normal distance from each reference curve to the target curve. The variables a' and b' are then used in a weighted average with the displacement values of the reference curves. A new displacement value is generated that will produce the target strain value at the corresponding increment. The relationship between the weighted average and the displacement path is:

$$(d_{22})_* = (d_{22})_1 + \frac{a'}{a' + b'} L \quad (2)$$

Figure 1b shows the visual interpretation of this relationship. This updated displacement path, when applied to the cruciform specimen in the FE simulations, will result in a linearized strain path that will be closer to the target strain ratio previously identified.

3. FINITE ELEMENT MODEL

The results presented in this paper are based on a FE model analyzed using Abaqus/Standard 2019. The cruciform specimen geometry was previously optimized [5], features notched corners, and a reduced pocket thickness of 0.53mm from the 2.93mm original sheet thickness as seen in Figure 2. To save on computation time, only 1/8th of the full cruciform geometry was modeled with two-fold symmetries. Displacement boundary conditions along the x- and y-direction were applied at the end of the specimen arms with amplitudes at each time increment. The model was meshed using fully integrated hexahedral elements, with a higher concentration of elements in the pocket area where the deformation was concentrated. Four elements were assigned through the thickness direction. The strain data used for the interpolation was collected as an average of the center gauge area within the diameter of 5.33 mm (highlighted in red in Figure 2), which is roughly halfway between the center of the pocket and

bottom of the fillet. The material used in this model was AISI 1008 steel with a Young's modulus of 210,000 MPa and Poisson's ratio of 0.3. The plastic material properties were previously determined experimentally (red solid) and extrapolated to a strain of 1 (red dash) [5] in Figure 3.

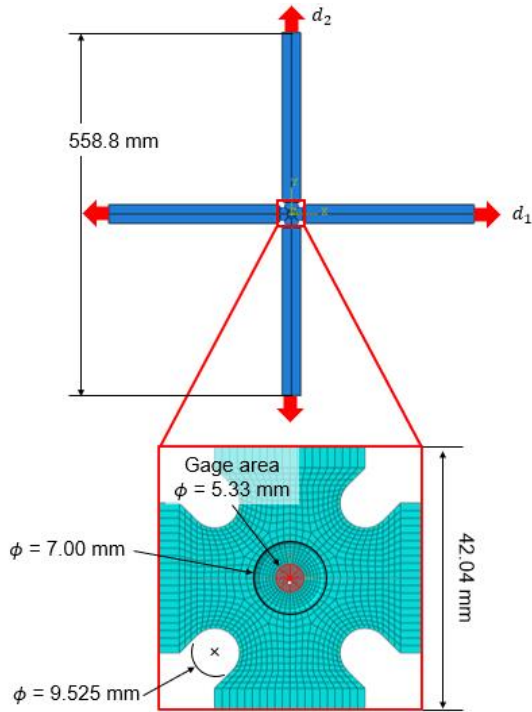


FIGURE 2: FE MODEL OF CRUCIFORM GEOMETRY

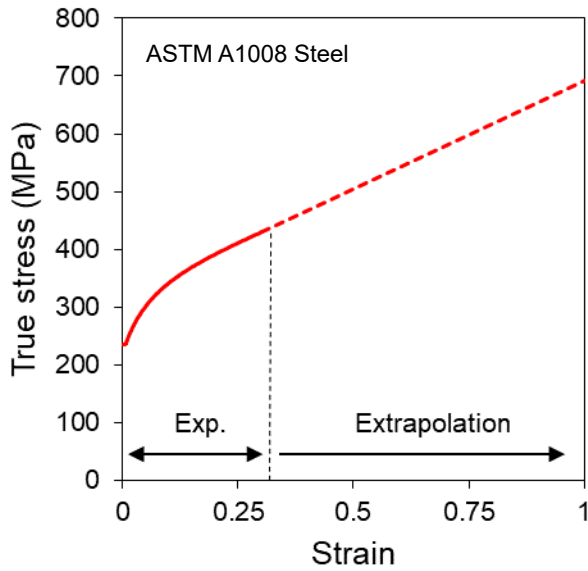


FIGURE 3: ASTM A1008 STEEL (EQUIVALENT TO AISI 1008 STEEL) STRESS-STRAIN CURVE FOR PLASTIC PROPERTIES.

4. DOUBLE INTERPOLATION

Figure 4 shows an example of the input and output strain paths of the interpolation method. The selected target strain path

in this paper is plane strain, i.e., $\epsilon_{22} \approx 0$, which follows the y-axis in the strain plot. To begin the process, initial reference strain paths were generated for three linear displacement paths, i.e., $d_{11}:d_{22} = 2:-0.4$ (green dotted), $2:0.5$ (red dash), and $2:1$ (purple dot dash), by FE simulations for the cruciform model (Figure 4). The resulting strain paths from the simulations were non-linear and not close to the plane strain target. These strain paths then served as the reference curves in the interpolation process to produce a linear strain path for a plane strain condition.

Since the strain path of $2:0.5$ (red dash) crosses the target plane strain path (black solid), the interpolation method was applied in two parts with different sets of reference curves. For the first part, before the strain path of $2:0.5$ intersects the plane strain target, the strain paths of $2:0.5$ and $2:1$ were used for the interpolation. Then, for the second part, curves $2:-0.4$ and $2:0.5$ were used.

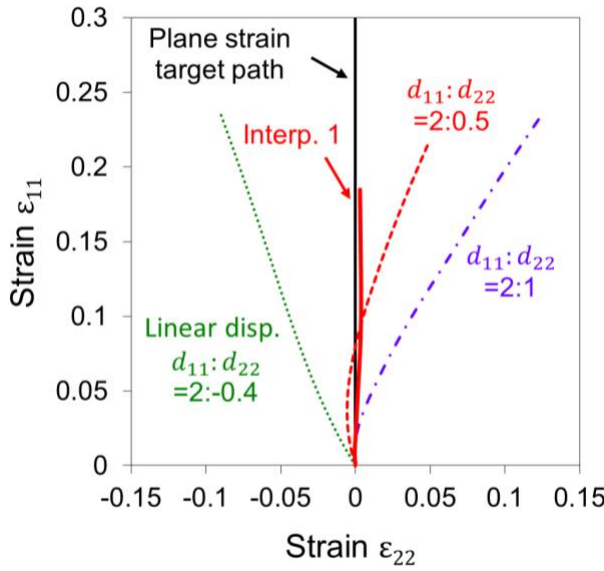


FIGURE 4: RESULTS OF INITIAL INTERPOLATION OF PLANE STRAIN PATH (FROM RED DASH TO RED SOLID LINE) USING PAIRS OF THE THREE REFERENCE CURVES SHOWN.

The result of the interpolation is shown as the solid red line in Figure 4. While the path shows increased linearity and is close to the targeted path, there is a visible difference with the target due to the non-linearity at the beginning. Thus, it is proposed to interpolate a second time, named as double interpolation here, to get even closer to the target. In this second iteration, the result of the first interpolation (red solid in Figure 4) was used as one of the reference curves instead of the $2:1$ path.

Figure 5 shows the result of the second interpolation (blue solid) with two references (green dotted and red solid) and target path (black solid). It should be noted that the strain path for $r = -5$ (strain ratio $2:-0.4$) was also interpolated during the first interpolation and the updated path (green dotted in Figure 5) was used to improve the result in the second interpolation iteration plane strain path. Compared to the single interpolation,

the result of double interpolation shows much improved linearity and is closer to the target plane strain path.

Figure 6 shows the corresponding displacement paths that were obtained from this interpolation progression. The red dash line represents the initial linear displacement path of 2:0.5, the red and blue solid lines are the results of the single and double interpolations (first and second iterations), respectively. These displacement paths represent a progression towards approaching the desired linear plane strain path.

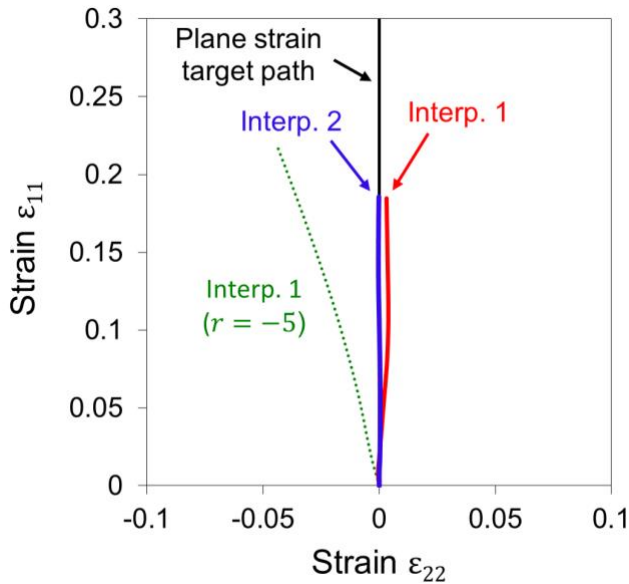


FIGURE 5: RESULTS OF DOUBLE INTERPOLATION (BLUE SOLID LINE) COMPARED TO SINGLE INTERPOLATION (RED SOLID LINE) AND TARGET PATH (BLACK SOLID LINE).

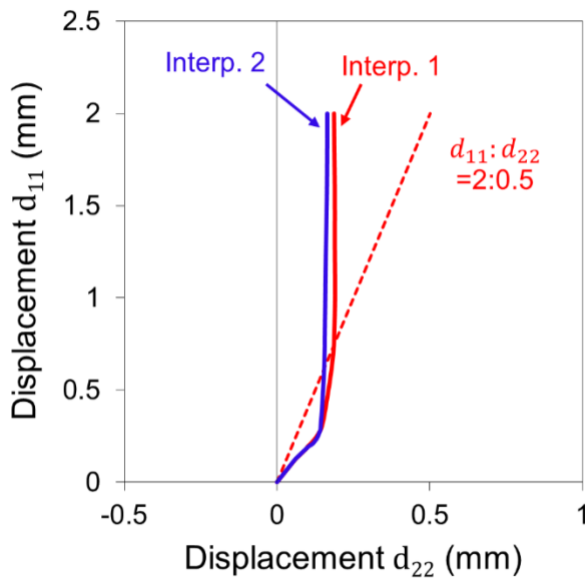


FIGURE 6: DISPLACEMENT PATH COMPARISON OF DOUBLE INTERPOLATION (BLUE SOLID LINE), SINGLE INTERPOLATION (RED SOLID LINE), AND LINEAR (RED DASH LINE).

5. CONCLUSION

Through a progression from linear input displacement to single and double interpolated outputs, it has been shown that the interpolation method can achieve results closer to the target path, in this case a plane strain forming condition. This result has great implications to biaxial tension testing for users to produce a desired strain path through the displacement control. Future work will include experiments to validate the success of this method by applying the optimized displacement path into the experimental set up. The strain will be measured by a surface 3D stereo digital image correlation (stereo-DIC) system and compared to the simulated results.

ACKNOWLEDGEMENTS

Support from the National Institute of Standards and Technology, through the Summer Undergraduate Research Fellowship (SURF) program, and funding for the NH BioMade Project from the U.S. National Science Foundation EPSCoR award (#1757371) are gratefully acknowledged.

DISCLAIMER

Certain commercial software, equipment, or materials are identified in this paper in order to specify the experimental procedure adequately. Such identification is not intended to imply recommendation or endorsement by the National Institute of Standards and Technology, nor is it intended to imply that the software, materials, or equipment identified are necessarily the best available for the purpose.

REFERENCES

- [1] Hoffman, J., Banerjee, D., Iadicola, M., "Determination of Strain Path Envelope in an Optimized Biaxial Cruciform Specimen of AISI 1008 Steel under Linear, Bilinear, and Nonlinear Strain Paths", *The Materials Society Conference 2022*
- [2] Banerjee, Dilip, Mark Iadicola, Adam Creuziger, and Timothy Foecke. "An experimental and numerical study of deformation behavior of steels in biaxial tensile tests." *In TMS 2015 144th Annual Meeting & Exhibition*, pp. 279-288. Springer, Cham, 2015
- [3] Deng, N., Kuwabara, T., Korkolis, Y.P., "Cruciform Specimen Design and Verification for Constitutive Identification of Anisotropic Sheets," *Experimental Mechanics*, 55, 6, 1005-1022, 2015
- [4] Yanaga, D., Kuwabara, T., Uema, N., Asano, M. "Material modeling of 6000 series aluminum alloy sheets with different density cube textures and effect on the accuracy of finite element simulation." *International Journal of Solids and Structures*, 49 25, 3488-3495, 2012
- [5] Creuziger, A., Iadicola, M., Foecke, T., Rust, E., and Banerjee, D., 2017, "Insights into Cruciform Sample Design," *JOM*, 69(5), pp. 902-906.